

STAR RESULTS FROM THE FIRST RHIC YEAR

RENE BELLWIED FOR THE STAR COLLABORATION

Physics Department, Wayne State University, Detroit, MI 48201, U.S.A.

An overview is presented of the results of the STAR experiment from the analysis of Au+Au collisions at $\sqrt{s_{NN}} = 130$ GeV acquired during the first year of RHIC operation. The transverse momentum distribution of negative hadrons has been studied out to 6 GeV/c in central Au+Au collisions and elliptic flow measurements out to 4.5 GeV/c in non-central collisions. This allows us to study hard processes and potentially effects of nuclear matter on parton propagation. Soft processes, which dominate particle production below around 2 GeV/c, have also been studied through the identified spectra of kaons, \bar{p} , and strange baryons.

1 The STAR experiment and its physics goals

The recent announcement of indirect evidence for the formation of a new state of matter in several CERN heavy-ion experiments has led to renewed interest for the field of relativistic heavy-ion collisions. In its first run, the Relativistic Heavy Ion Collider (RHIC) at the Brookhaven National Laboratory collided Au ions at a center of mass energy of 130 GeV per nucleon pair, some 7.5 times higher than that previously possible in fixed target experiments at CERN. The ultimate goal of experiments is to establish the existence of a deconfined phase of quarks and gluons and to study the behaviour of strongly interacting matter under these conditions. As expected, the very first measurements reported from RHIC were based on hadronic observables. Thermal model descriptions of hadronic particle production at CERN, in particular the strange particle abundances and ratios, have concluded that only the inclusion of a phase transition into any model calculation will allow a proper description of the measured results¹. In addition, particle production at high transverse momentum (p_T) is expected to become more pronounced at RHIC energies. High p_T particles originate from hard processes occurring during the earliest stages of the collision and may therefore offer new insight into the state of matter produced.

The Solenoidal Tracker At RHIC (STAR) detector is a large acceptance spectrometer primarily designed to study hadron production in nuclear collisions ranging from proton-proton to central Au+Au. During the first year of operation, the STAR detector comprised a central Time Projection Chamber (TPC), a Ring Imaging Cherenkov (RICH), a Central Trigger Barrel (CTB) and two Zero Degree Calorimeters (ZDC). The TPC operated in a 0.25 Tesla solenoidal magnet and gives tracking information for charged particles in a

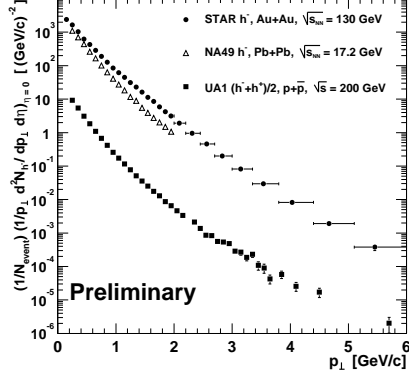


Figure 1. The negative hadron p_T distribution from the 5% most central collisions. Also shown is the same distribution measured in Pb+Pb collisions at $\sqrt{s_{NN}} = 17.2$ GeV and average charge hadron yield from $p+\bar{p}$ collisions at $\sqrt{s} = 200$ GeV.

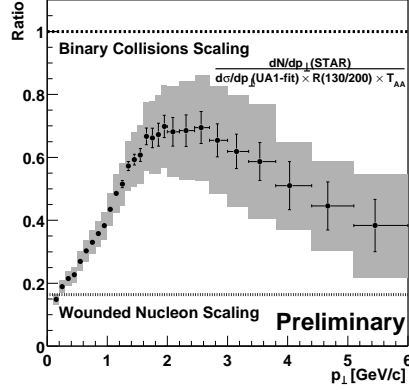


Figure 2. Ratio of the STAR and scaled UA1 p_T spectra. The vertical error bars indicate the measurement error, the shaded region the total uncertainty including that of the scaling factors applied to the UA1 data.

pseudorapidity interval of approximately $|\eta| < 1.8$. It also provides a means of particle identification from ionisation (energy loss) measurements along each particle trajectory. Particle identification at higher momenta was made possible using the RICH. The RICH covers only a narrow acceptance window centered at mid-rapidity ($\Delta\phi = 20^\circ$ in azimuth and $|\eta| < 0.3$), thus its measurements in year-1 were statistics limited. Overall about 500,000 Au+Au collisions (central and minimum bias) recorded with the STAR detector in year-1 were analyzed for the results shown here. The detector was triggered using the signals from the CTB and ZDCs.

2 Results

Fig. 1 shows the inclusive transverse momentum distribution of negative hadrons measured out to $p_T = 6$ GeV/c. The data shown are for the 5% most central event. The data has been corrected for background arising from interactions in the detector and the products of weak decay processes, as well as for losses due to the reconstruction efficiency.

Also shown in Fig. 1 is the negative hadron distribution from Pb+Pb collisions at $\sqrt{s_{NN}} = 17.2$ GeV of NA49 ² and the distribution of charged hadrons $(h^- + h^+)/2$ from proton-antiproton collisions at $\sqrt{s} = 200$ GeV of UA1 ³. It can be seen that the STAR data is flatter than that measured in Pb+Pb collisions at lower energy, corresponding to an increase in the mean p_T of negative hadrons by 18%. The total yield, which was obtained by extrapolation of a power-law fit to the data ⁴, was found to be $dN/d\eta|_{\eta=0} = 280 \pm 1(stat) \pm 20(syst)$, a 52% increase compared to the NA49 measurement. In order to compare to the proton-antiproton data, Fig. 2 shows the ratio of the STAR data to a scaled parametrisation of the UA1 data. The UA1 data has been scaled to account for the energy difference in the nucleon-nucleon centre-of-mass frame and by the nuclear overlap integral, $T_{AA} = 26 \text{ mb}^{-1}$, ⁴ to arrive at the yield appropriate for the number of binary nucleon-nucleon collisions expected in central Au+Au collisions. The horizontal lines shown in Fig. 2 correspond to the expected value of the ratio under two scaling assumptions. The upper line shows the expected value if the distribution scales with the number of binary collisions. This line corresponds to a ratio of unity due to the scaling of the UA1 data. The lower line corresponds to the expected value of the ratio if the distributions scale with the number of wounded nucleons. As expected, at low p_T , where particle production is dominated by soft processes, the total pion yield scales with the number of wounded nucleons. However, this is only the case for the lowest transverse momentum bin. In general, the data below $p_T = 2$ GeV/ c exceeds the wounded nucleon scaling, rising as a function of p_T toward the binary collision limit. This upper limit is relevant for hard processes in the absence of any nuclear effects, such as initial state multiple scattering, jet quenching or collective radial flow. In fact, the ratio never reaches the binary collision scaling, but drops again for $p_T > 2$ GeV/ c . At a p_T of 6 GeV/ c , the ratio falls below the binary collision scaling by more than a factor of two. A second measurement that may be sensitive to high p_T phenomena is elliptic flow. Elliptic flow is studied in minimum bias collisions, where the initial spatial anisotropy caused by the partial overlap of two nuclei is transformed into a momentum anisotropy of particles in the final state. For each event a reaction plane is determined from the predominantly low p_T tracks reconstructed in the TPC ⁵. Particle distributions are then studied for an azimuthal asymmetry with respect to the reaction plane, which may stem from pressure gradients generated in the earliest stages of the collision. Fig. 3 shows the second Fourier coefficient, v_2 , of the azimuthal distribution of negative hadrons as a function of p_T . The data shows that v_2 rises as a function of p_T , as expected from hydrodynamic calculations ⁶, until around $p_T = 2$ GeV/ c where-after the data

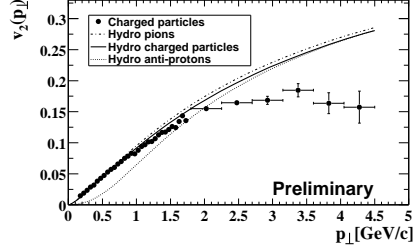


Figure 3. v_2 as function of p_T , compared to hydrodynamical calculations (see text for details).

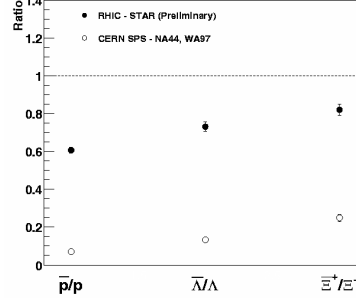


Figure 4. Anti-baryon to baryon ratios measured by STAR, ordered by strangeness content and compared to values obtained at the SPS.

falls systematically below the hydrodynamical prediction. This departure is not unexpected as high p_T particles may escape the reaction zone with little rescattering. However, v_2 appears to saturate rather than decrease and this may be related to the in-medium energy loss of high p_T partons. Calculations have shown that in this case the magnitude of v_2 is sensitive to the initial gluon density ⁷.

It is tempting to connect the two observations seen in Figs. 1 and 3. In Fig. 1 a suppression of high p_T hadrons is observed in Au+Au collisions relative to scaled $p+\bar{p}$ data, while in Fig. 3 the anisotropic flow signal is found to saturate at high p_T , both of which may be the result of partonic energy loss (jet quenching) in the excited medium.

Particle identification in STAR can be performed in three ways: using the specific ionisation (dE/dx) in the TPC, from the angle at which Cherenkov light is emitted from particles entering the RICH, and by the topology of weak decays reconstructed from the tracks in the TPC. At a given momentum, the difference in the mean ionisation between particle species allows the separation of pions and kaons for momenta $p \leq 0.6$ GeV/ c and the separation of kaons and protons for momenta $p \leq 1.0$ GeV/ c . The RICH extends the particle identification capability of the TPC to around 3 GeV/ c for kaons and 5 GeV/ c for protons. The topological pattern recognition technique is applicable to a wide range of weak decay processes, from neutral strange particle decays such as $K_s^0 \rightarrow \pi^+ + \pi^-$ and $\Lambda \rightarrow p + \pi^-$, to cascade decay processes such as

$\Xi^- \rightarrow \Lambda + \pi^-$ and one-prong decays such as $K^- \rightarrow \mu^- + \nu_\mu$.

Fig. 4 shows the anti-particle over particle ratios for identified baryons at mid-rapidity in the 11% most central collisions. The ratios indicate that the mid-rapidity region is not net baryon free, although comparisons with measurements at SPS energies indicate that the net baryon density is much reduced. The ratios are consistent with simple quark counting models⁸ and statistical thermal models which are governed by a common baryon chemical potential and chemical freeze-out temperature⁹. The ratios shown in Fig. 4 are based on integrated yields, which are easy to obtain in the case of the strange baryons, where the topological pattern recognition allows to cover around 70% of the particle's momentum spectrum. In the case of the \bar{p}/p ratio the coverage based on the energy loss technique is much smaller due to the rather low momentum cutoff ($p \leq 1$ GeV/c). Still, an extrapolation was done and the details can be found at¹⁰. The particle identified transverse mass distributions of negative hadrons (π^- , K^- and \bar{p}) obtained by the dE/dx method in the 6% most central collisions were compared to an exponential fit. A clear mass dependence was observed in the inverse slope parameter, with values ranging from 190 MeV for π^- to 300 MeV for K^- and 565 MeV for \bar{p} . These observations are suggestive of a significant increase in transverse radial flow compared to CERN observations^{2,11}. Unfortunately the transverse mass range obtained from the dE/dx measurement is very limited, especially for the \bar{p} . The transverse momentum spectra of h^- , \bar{p} and $\bar{\Lambda}$ are shown in Fig. 5.

It is noteworthy that the inverse slope obtained from an exponential fit to the $\bar{\Lambda}$ spectrum is significantly lower than that of the \bar{p} spectrum. One of the consequences of radial flow is a flattening of the transverse momentum spectra for heavier particles at low p_T ¹². Therefore the slope obtained from a simple exponential fit to the data will be dependent on the range of p_T used in the fit. Fig. 5 also suggests that the relative yield of $\bar{\Lambda}$ to negative hadrons becomes increasingly larger at higher p_T . It should be noted that the negative hadron distribution already contains the yield of primary antiprotons. If this trend continues, then it would appear that the yield of antibaryons may exceed that of mesons at transverse momenta above 2 GeV/c. This is in qualitative agreement with the direct measurement of the \bar{p}/π^- reported by the PHENIX collaboration¹³. A detailed study of baryon production in year-2 may determine whether this observation is solely a consequence of transverse radial flow, or due to novel baryon dynamics¹⁴.

In an attempt to remove the dependence of the fit range and seek a common explanation for the spectra, a hydrodynamical motivated fit¹⁵ has been performed. The model allows a choice of the transverse flow profile of matter produced in the collision. The choice which best describes the

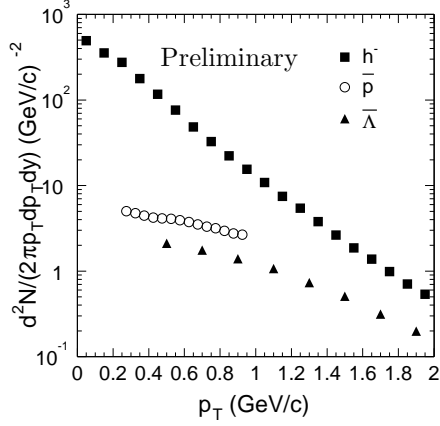


Figure 5. The transverse mass spectra of h^- , \bar{p} and $\bar{\Lambda}$ in the 11% most central events.

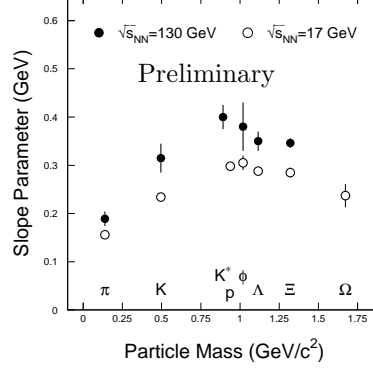


Figure 6. The mass dependence of the slope parameters obtained from exponential fits to the transverse mass distribution of strange particles in the central Au-Au collisions (statistical errors only).

data is a radial flow velocity which varies as $\beta_r = \beta_s \sqrt{r/R}$ where β_s is the surface flow velocity at a radius, R . A fit was performed to each of the particle spectra, allowing the freezeout temperature and mean flow velocity to vary. It was found that a freezeout temperature of $T = 120^{+50}_{-25}$ MeV and an average flow velocity of $\beta_r = 0.52^{+0.12}_{-0.08}$ could simultaneously describe all measured particle spectra. These values represent a modest rise in the transverse flow velocity and similar freezeout temperature compared to earlier measurements at CERN^{2,11}. For the strange particles reconstructed in STAR (including the Kaon kink analysis, which extends the m_T coverage up to 2 GeV/c) the coverages are similar and a simple exponential fit can be applied in order to yield a common mass dependence. The result is shown and compared to SPS data in Fig. 6.

3 Summary

In summary, STAR has measured a wide range of hadronic probes in both central and minimum bias Au+Au collisions at $\sqrt{s_{NN}} = 130$ GeV. The pseudorapidity density of negative hadrons is $dN/d\eta = 280 \pm 1 \pm 20$ in central collisions, representing a 52% increase compared to lower energy data from

CERN. The elliptic flow measurement in minimum bias collisions is consistent with the predictions of a hydrodynamical model at low transverse momentum, implying that the system equilibrates early. Studies of the transverse momentum spectra of identified particles produced in central collisions indicate the presence of a strong collective radial flow, which complicates the interpretation of transverse momentum spectra. However, a common description of the spectra is possible within a hydrodynamical framework. At transverse momenta greater than 2 GeV/ c there is a suppression of negative hadrons compared to an extrapolation from proton-antiproton collisions. The elliptic flow measurement is also found to saturate in this momentum region. Both observations may be sensitive to partonic energy loss (jet quenching) at this higher energy. Finally it has been shown that antibaryons (and baryons) become an increasingly larger fraction of the total particle yield at high p_T .

References

1. U. Heinz, Nucl.Phys. **A661** 140c (1999).
2. H. Appelshäuser *et al.*, Phys. Rev. Lett. **82** 2471 (1999).
3. C. Albajar *et al.*, Nucl. Phys. **B355** 261 (1990).
4. C. Adler *et al.*, Phys. Rev. Lett. **87** 112303 (2001).
5. K.H. Ackermann *et al.*, Phys. Rev. Lett. **86** 402 (2001).
6. P. Huovinen *et al.*, Phys. Lett. **B503**, 58 (2001).
7. M. Gyulassy, I. Vitev and X.N. Wang, Phys. Rev. Lett. **86** 2537 (2001).
8. J. Zimanyi *et al.*, Phys. Lett. **B472** 243 (2000).
9. P. Braun-Munzinger *et al.*, Phys. Lett. **B518** 41 (2001).
10. C. Adler *et al.*, Phys. Rev. Lett. **86** 4778 (2001).
11. F. Antinori *et al.*, Nucl. Phys. **A661**, 841c (1999).
12. P. Siemens and J.O. Rasmussen, Phys. Rev. Lett. **42**, 880 (1979).
13. W. Zajc for PHENIX, QM 2001 proc., Nucl. Phys. **A698** (2002).
14. I. Vitev and M. Gyulassy, nucl-th/0104066.
15. E. Schnedermann *et al.*, Phys. Rev. **C48** 2462 (1993).